Search for Cell Motility and Angiogenesis Inhibitors with Potential Anticancer Activity: Beauvericin and Other Constituents of Two Endophytic Strains of *Fusarium oxysporum*[1]

Jixun Zhan,[†] Anna M. Burns,[†] Manping X. Liu,[†] Stanley H. Faeth,[‡] and A. A. Leslie Gunatilaka*[,†]

SW Center for Natural Products Research and Commercialization, Office of Arid Lands Studies, College of Agriculture and Life Sciences, The University of Arizona, 250 East Valencia Road, Tucson, Arizona 85706-6800, and School of Life Sciences, College of Liberal Arts and Sciences, Arizona State University, Tempe, Arizona 85287-4501

Received August 10, 2006

Wound-healing assay-guided fractionation of an EtOAc extract of the fungal strain *Fusarium oxysporum* EPH2R$_{AA}$ endophytic in *Ephedra fasciculata* afforded beauvericin (**1**), (−)-oxysporidinone (**2**), and two new *N*-methyl-2-pyridones, (−)-4,6′-anhydrooxysporidinone (**3**) and (−)-6-deoxyoxysporidinone (**4**). Beauvericin (**1**) inhibited migration of the metastatic prostate cancer (PC-3M) and breast cancer (MDA-MB-231) cells and showed antiangiogenic activity in HUVEC-2 cells at sublethal concentrations. Cytotoxicity-guided fractionation of an EtOAc extract of *F. oxysporum* strain CECIS occurring in *Cylindropuntia echinocarpus* afforded rhodolamprometrin (**5**), bikaverin (**6**), and the new natural product 6-deoxybikaverin (**7**). All compounds were evaluated for cytotoxicity in a panel of four sentinel cancer cell lines, NCI-H460 (non-small-cell lung), MIA Pa Ca-2 (pancreatic), MCF-7 (breast), and SF-268 (CNS glioma), and only beauvericin (**1**) and bikaverin (**6**) were active, with **1** and **6** showing selective toxicity toward NCI-H460 and MIA Pa Ca-2, respectively. Interestingly, 6-deoxybikaverin (**7**) was completely devoid of activity, suggesting the requirement of the C-6 hydroxy group of bikaverin for its cytotoxic activity.

Cancer chemotherapy has relied mostly on cytotoxic drugs, which inhibit tumor cell proliferation and cause cell death. In recent years targeting cell motility has attracted attention as one of the alternative strategies for the development of anticancer therapies.[2] Metastasis is reported to be responsible for over 90% of cancer deaths.[3] Cell motility (migration) is a critical cause of tissue invasion allowing primary tumors to disseminate and metastasize. Cell migration is also involved in a number of physiological processes including ovulation, embryonic development, tissue regeneration (wound healing), and inflammation. These migration activities of cells in vitro are thought to be related to many in vivo cellular behaviors such as tumor angiogenesis, cancer cell invasion, and metastasis.[4] It is known that primary solid tumors depend on angiogenesis (formation of new blood vessels) to obtain the necessary oxygen and nutrients for growth beyond a certain size (ca. 1−2 mm). The transition from a pre-angiogenic condition to tumor angiogenesis, often referred to as the angiogenic switch, is followed by tumor growth, cancer cell invasion, and metastasis. It should therefore be possible to halt (or retard) this process at different stages with the help of cell motility inhibitors. Cell motility under ordinary physiological conditions in an adult is rather infrequent; its repression might therefore be accompanied by manageable toxicity.[5] Small-molecule inhibitors have been used to study the migration of living cells, and it was found that the most readily available compounds directly disrupt actin microfilaments or microtubules.[6] Several small-molecule natural products such as withaferin A,[7] prodigiosin,[8] and migrastatin[9] have been reported to inhibit cell motility. Of the methods available to screen natural product libraries/extracts for cell motility inhibitors, a moderate throughput assay known as the wound-healing assay (WHA) employing metastatic cancer cell lines has gained popularity due to its simplicity. Utilization of this assay has led to the discovery of motuporamines, capable of inhibiting angiogenesis,[10] and the Rho-kinase inhibitor 3-(4-pyridyl)indole (Rockout).[11]

Recent studies have demonstrated that plant-associated microorganisms are prolific producers of novel and pharmacologically active secondary metabolites.[12] In the course of our ongoing efforts to discover potential anticancer agents from Sonoran desert plants and their associated microorganisms,[1] EtOAc extracts derived from two endophytic strains of *Fusarium oxyporum* (mitosporic Hypocreales) inhabiting the root tissue of *Ephedra fasciculata* (Mormon tea; Ephedraceae) and the stem tissue of *Cylindropuntia echinocarpus* (silver cholla; Cactaceae) were found to have activity in WHA and the MTT (tetrazolium-based colorometric) assay[13] for cancer cell proliferation/survival. WHA-guided fractionation of an EtOAc extract of a solid culture of *F. oxysporum* strain EPH2R$_{AA}$ led to the isolation of beauvercin (**1**), along with (−)-oxysporidinone (**2**) and two of its new analogues, (−)-4,6′-anhydrooxysporidinone (**3**) and (−)-6-deoxyoxysporidinone (**4**). MTT assay-guided fractionation of an EtOAc extract of a liquid culture of *F. oxysporum* strain CECIS led to the isolation of rhodolamprometrin (**5**), bikaverin (**6**), and the new natural product 6-deoxybikaverin (**7**). Known to be a plant pathogen, *F. oxysporum* has been previously subjected to a number of investigations that has resulted in the isolation of several bioactive metabolites including fumonisins, oxysporidinone, sambutoxin, and cyclosporine A.[14] Beauvericin (**1**) has previously been encountered in a number of fungal strains including *Beauveria bassiana*,[15a] *Paecilomyces fumoso-roseus*,[15b] *Polyporus sulphureus*,[15c] *Fusarium semitectum*,[16a] and *F. moniliforme* var. *subglutinans*;[16a] beauvericin has been detected in fruit tissues of two cultivars of melon fruits artificially infected with a strain of *F. oxysporum* f. sp. *melonis*.[16b] In addition to its well-characterized entomopathogenic activity,[16] **1** has been reported to be toxic to the brine shrimp, *Artemia salina*,[15a] and two human cell lines, Hep G2 (hepatocellular carcinoma) and MRC-5 (fibroblast-like fetal lung cells),[17] to possess anticonvulsion and antiarrhythmic activities, induce apoptosis in several cancer cell lines, and to inhibit acyl-CoA (cholesterol acyltransferase activity).[18] It has recently been suggested that the induction of apoptosis by beauvericin (**1**) involves multiple cellular/molecular pathways including pro- and antiapoptotic Bcl-2 family proteins, mitochondrial membrane potential, mitochondrial cytochrome *c*, and caspase 3.[19] Bikaverin (**6**) has been reported to be cytotoxic to Erlich ascites carcinoma, leukemia L5178, and sarcoma 37 cells probably by inhibiting nucleic acid and protein synthesis.[20]

* To whom correspondence should be addressed. Tel: (520) 741-1691. Fax: (520) 741-1468. E-mail: leslieg@ag.arizona.edu.

[†] SW Center for Natural Products Research and Commercialization, University of Arizona.

[‡] Arizona State University.

10.1021/np060394t CCC: $37.00
Published on Web 02/08/2007

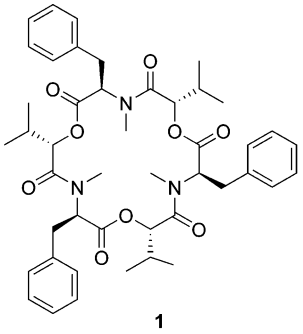

1

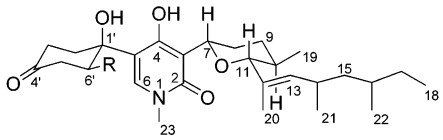

2 R = OH
4 R = H

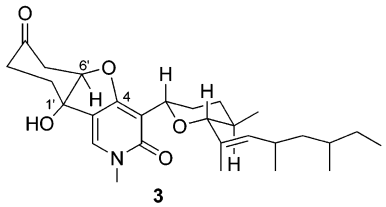

3

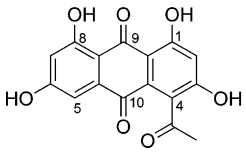

5

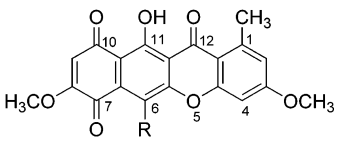

6 R = OH
7 R = H

Results and Discussion

The EtOAc extract of *F. oxysporum* strain EPH2R$_{AA}$ exhibiting activity in wound-healing assay (WHA), on bioassay-guided fractionation involving solvent−solvent partitioning followed by Sephadex LH-20 size-exclusion and silica gel chromatography afforded **1**−**4**. Compound **1** was identified as beauvericin by comparison of its mass and NMR spectral data with those reported[15] for this cyclic hexadepsipeptide. ^{1}H and ^{13}C NMR data (Tables 1 and 2) together with its mass spectrum suggested compound **2** to be identical with (+)- or (−)-oxysporidinone previously encountered in *F. oxysporum* strains CBS 330.95[14d] and N17B,[14f] respectively. However, the optical rotation observed for **2** ([α]$_D$ −101) confirmed it to be (−)-oxysporidinone.[14f] Although the application of ^{1}H−^{1}H coupling constants and NOE data has aided the determination of relative orientation of groups on cyclohexanone and pyran rings of (+)-oxysporidinone, the absence of NOE interactions between protons of these two moieties has precluded determination of complete relative stereochemistry for this compound.[14d] Compound **3** was determined to have the molecular formula $C_{28}H_{41}NO_5$. Its ^{1}H and ^{13}C NMR data (Tables 1 and 2) were similar to those of **2** except for the chemical shifts in the neighborhood of C-4 and C-6′. In the ^{13}C NMR spectrum of **3**, compared with compound **2**, the signal due to C-4 was shifted from δ 163.7 to δ 168.5 and that for C-6′ from δ 71.5 to δ 92.0, indicating that a molecule of H_2O may have been lost from the two hydroxyl groups at these positions in **2** to form an ether linkage. The coupling constant (4.3 Hz) observed for H-6′ suggests that this proton is equatorial.[14f] The ^{1}H NMR spectrum of **3** when recorded in DMSO-d_6 showed, in addition to other signals, only one D_2O exchangeable signal, which appeared as a sharp singlet at δ 6.00, and this was assigned to 1′-OH. The absence of a signal around δ 10.0 due to 4-OH in its ^{1}H NMR spectrum in DMSO-d_6 further supported that this OH had participated in the formation of an ether linkage. The HMBC correlations of H-6′ with C-4 and C-4′ (Figure 1) confirmed the presence of the C-4−O−C-6′ linkage in **3**. On the basis of COSY, HSQC, and HMBC spectra, the structure of **3** was established as (−)-4,6′-anhydrooxysporidinone. Spectroscopic data of compound **4** indicated that it is structurally related to **2** and **3**. The molecular formula of **4** was determined to be $C_{28}H_{43}NO_5$ from HRFABMS, suggesting that it has one oxygen atom less than oxysporidinone (**2**). However, its ^{13}C NMR spectrum exhibited only 27 signals, with a strong signal at δ 36.8 due to the overlapping signals of two CH_2 groups as indicated by DEPT, ^{1}H NMR, and HSQC spectra. Compared with

Table 1. ^{1}H NMR Data (500 MHz) for Compounds **2**−**4**

	δ_H multiplicity (*J* in Hz)		
position	**2**[a]	**3**[a]	**4**[b]
4-OH			10.5 s
6	7.68 s	7.68 s	7.06 s
7	4.90 dd (11.2, 2.0)	4.76 dd (11.7, 2.3)	4.95 dd (11.1, 2.0)
8	1.94, 1.65 m	2.18, 1.53 m	2.06 m
9	1.93, 1.42 m	1.90, 1.31 m	1.90, 1.42 m
10	1.75 m	1.65 m	1.70 m
11	3.54 m	3.37 m	3.50 m
13	5.24 d (9.4)	5.11 dd (9.5, 1.1)	5.21 d (9.0)
14	2.55 m	2.51 m	2.49 m
15	1.24, 1.09 m	1.22, 1.08 m	1.21, 1.04 m
16	1.33 m	1.36 m	1.30 m
17	1.42, 1.06 m	1.43, 1.08 m	1.34, 1.04 m
18	0.85 m[c]	0.85 m[d]	0.83 m[e]
19	0.78 d (6.6)	0.73 d (6.6)	0.75 d (6.6)
20	1.66 s	1.57 d (1.1)	1.65 s
21	0.93 d (6.6)	0.90 d (6.6)	0.92 d (6.3)
22	0.85 m[c]	0.85 m[d]	0.83 m[e]
23	3.51 s	3.51 s	3.44 s
2′	2.60, 1.85 m	2.33, 2.25 m	2.38, 2.13 m
3′	2.78, 2.15 m	2.38, 2.03 m	2.90, 2.28 m
5′	2.83, 2.47 m	3.48 brd (11.0) 3.37 brd (11.0)	2.90, 2.28 m
6′	4.54 dd (11.4, 5.3)	4.92 d (4.3)	2.38, 2.13 m

[a] In CD_3OD. [b] In $CDCl_3$. [c−e] Overlapping signals.

Table 2. ^{13}C NMR Data (125 MHz) for Compounds **2**−**4**

	δ_C, multiplicity[a]		
position	**2**[b]	**3**[b]	**4**[c]
2	163.3, C	165.3, C	161.1, C
3	111.2, C	109.5, C	111.2, C
4	163.7, C	168.5, C	162.0, C
5	118.1, C	119.1, C	117.2, C
6	138.4, CH	135.8, CH	133.0, CH
7	79.1, CH	73.7, CH	78.1, CH
8	31.5, CH_2	30.3, CH_2	30.6, CH_2
9	33.2, CH_2	34.1, CH_2	32.0, CH_2
10	33.7, CH	33.1, CH	32.5, CH
11	93.6, CH	93.2, CH	92.5, CH
12	132.0, C	133.9, C	130.0, C
13	138.7, CH	137.4, CH	138.1, CH
14	30.9, CH	30.9, CH	29.7, CH
15	46.1, CH_2	46.4, CH_2	44.7, CH_2
16	33.4, CH	33.4, CH	32.0, CH
17	29.8, CH_2	30.1, CH_2	28.9, CH_2
18	11.6, CH_3	11.7, CH_3	11.2, CH_3
19	18.0, CH_3	18.4, CH_3	17.6, CH_3
20	12.5, CH_3	11.7, CH_3	11.9, CH_3
21	21.2, CH_3	21.3, CH_3	20.7, CH_3
22	20.2, CH_3	20.2, CH_3	19.6, CH_3
23	37.8, CH_3	38.6, CH_3	37.2, CH_3
1′	74.8, C	77.2, C	70.2, C
2′	32.8, CH_2	34.4, CH_2	36.2[d], CH_2
3′	37.2, CH_2	36.0, CH_2	36.8, CH_2
4′	212.1, C	210.3, C	211.4, C
5′	47.0, CH_2	49.4, CH_2	36.8, CH_2
6′	71.5, CH	92.0, CH	36.3[d], CH_2

[a] Multiplicity from DEPT. [b] In CD_3OD. [c] In $CDCl_3$. [d] Interchangeable.

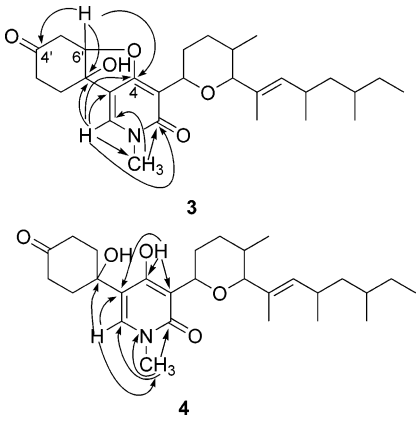

Figure 1. Selected HMBC correlations for **3** and **4**.

2 the ^{1}H NMR spectrum of **4** also exhibited an overlapping signal due to two CH_2 groups, which had cross-peaks to two methylene carbon signals at δ 36.2 and 36.3 in its HSQC spectrum. These two CH_2 groups were found to be attached to each other, as indicated by its COSY and HSQC spectra. Comparison of the NMR data of **4** with those of **2** suggested that in **4** the hydroxymethine group is replaced by a methylene group. Thus, compound **4** was identified as (−)-6′-deoxyoxysporidinone. Assignments of ^{1}H and ^{13}C NMR signals of **4** (Tables 1 and 2) have been made with the help of its 2D spectra, including the HMBC spectrum (Figure 1).

MTT assay-guided fractionation of a cytotoxic EtOAc extract of *F. oxysporum* strain CEC1S resulted in the isolation of compounds **5**−**7**. Compound **5** was identified as rhodolamprometrin by comparison of its mass and ^{1}H and ^{13}C NMR spectral data with those reported in the literature.[21] Compounds **6** and **7** exhibited very similar NMR spectra except for the absence of an OH group in **7** compared with **6**, as evident from their APCI-MS and ^{1}H NMR spectra. Spectroscopic data for **6** and **7** were found to be consistent with those reported for bikaverin[22] and 6-deoxybikaverin,[23] respectively. Rhodolamprometrin (**5**) has previously been isolated from the feather star, *Lamprometra klunzingeri*,[24] and a mutant of the deuteromycete *Trichoderma viride*.[21] Bikaverin (**6**) has been encountered in a number of microorganisms including several *Fusarium* species[25] and *Mycogone jaapii*.[26] 6-Deoxybikaverin (**7**) has previously been obtained only as a byproduct in the synthesis of bikaverin (**6**),[23] and this constitutes the first report of its natural occurrence.

Compounds **1**−**7** were evaluated for in vitro cytotoxic activity against a panel of four sentinel human cancer cell lines, NCI-H460 (non-small-cell lung), MIA Pa Ca-2 (pancreatic), MCF-7 (breast), and SF-268 (CNS glioma). Cells were exposed to serial dilutions of test compounds for 72 h in RPMI 1640 media supplemented with 10% fetal bovine serum, and when cell viability was evaluated by the MTT assay,[13] only beauvericin (**1**) and bikaverin (**6**) were found to be cytotoxic. The concentrations resulting in 50% inhibition of cell proliferation/survival as measured by the MTT assay (IC_{50}) were found to range between 0.01 and 1.81 μM (Table 3). Interestingly, 6-deoxybikaverin (**7**), which lacks the OH group at C-6, did not exhibit cytotoxic activity toward any of the cell lines used even at concentrations of 4.0 and 2.0 μg/mL. As beauvericin (**1**) was isolated using WHA-guided fractionation, it was evaluated for cell migration inhibitory activity in two metastatic cancer cell lines, PC-3M (prostate) and MDA-MB-231 (breast). Beauvericin (**1**) inhibited migration of PC-3M and MDA-MB-231 cells at concentrations ranging from 2.0 to 2.5 and 3.0 to 4.0 μM, respectively (Figure 2). The extent of cell migration inhibition when determined using NIH ImageJ software[27] suggested that **1** caused ca. 50% inhibition of the migration of PC-3M and MDA-MB-231 cells at concentrations of ca. 3.0 and 5.0 μM, respectively (Figure 3). The concentrations of **1** required for 50% (IC_{50}) and 25% (IC_{25}) inhibition of PC-3M cell proliferation/survival as measured by the MTT assay at 20 h (time used for WHA with PC-3M) were determined to be 3.8 and 2.3 μM, respectively, and those for MDA-MB-231 at 40 h (time used for WHA with MDA-MB-231) were found to be 7.5 and 6.4 μM, respectively, suggesting that it is capable of inhibiting migration of both metastatic cancer cell lines at sublethal concentrations. Encouraged by this observation we next evaluated the antiangiogenic activity of beauvericin (**1**) by assessing its ability to interfere with endothelial cell network formation.[28] Endothelial (HUVEC-2) cells in suspension were placed on top of a thin layer of Matrigel, allowing the cells to align and form tube-like structures. Cells were then exposed to vehicle control (DMSO) or increasing concentrations of **1** for 16 h, fixed, and observed under an inverted microscope. Beauvericin (**1**) clearly showed potent antiangiogenic activity at sublethal concentrations, as demonstrated by the inhibition of endothelial cell network formation (Figure 4); complete disruption of HUVEC-2 network formation was observed at a concentration (3.0 μM) below IC_{50} (7.5 μM) and IC_{25} (5.0 μM) of **1** for this cell type exposed for the same length of time (16 h). Studies to elucidate the molecular target(s) of beauvericin (**1**) by gene expression analysis and animal studies to evaluate its anticancer potential are currently in progress.

Table 3. Cytotoxicities of Compounds **1** and **6** against a Panel of Four Tumor Cell Lines[a]

	cell line[b]			
compound	NCI-H460	MIA Pa Ca-2	MCF-7	SF-268
1	1.41	1.66	1.81	2.29
6	0.43	0.26	0.42	0.38
doxorubicin	0.01	0.05	0.07	0.04

[a] Results are expressed as IC_{50} values in μM. [b]Key: NCI-H460 = human non-small-cell lung cancer; MIA Pa Ca-2 = human pancreatic carcinoma; MCF-7 = human breast cancer; SF-268 = human CNS cancer (glioma).

Experimental Section

General Experimental Procedures. Melting points were determined with an Electrothermal micromelting point apparatus and are uncorrected. Optical rotations were measured with a Jasco DIP-370 digital polarimeter using MeOH as solvent. IR spectra were recorded on a Shimadzu FTIR-8300 spectrometer in KBr disks and UV spectra in MeOH on a Shimadzu UV-1601 spectrometer. 1D and 2D NMR spectra were recorded on Bruker DRX-500 (500 MHz for ^{1}H NMR and 125 MHz for ^{13}C NMR) and Varian Inova-600 (600 MHz for ^{1}H NMR and 150 MHz for ^{13}C NMR) instruments. The chemical shift values (δ) are given in parts per million (ppm), and the coupling constants are in hertz. Low-resolution APCIMS were recorded on a Shimadzu LCMS-QP8000α HPLC-MS system, and high-resolution FABMS were obtained with a JEOL HX110A mass spectrometer.

Fungal Isolation, Identification, and Cultivation. The two endophytic strains of *F. oxysporum* used in this study were isolated from the root tissue of *Ephedra fasciculata* and the stem tissue of *Cylindropuntia echinocarpus* growing in the Sonoran desert and were deposited in the School of Life Sciences, Arizona State University, under the accession numbers $EPH2R_{AA}$ and CEC1S, respectively, and at the Southwest Center for Natural Products Research and Commercialization of the University of Arizona microbial culture collection under the accession numbers CS-36-33 and CS-69-50, respectively. Both strains were grown in small scale in solid (PDA) and liquid (PDB) media, processed as for large-scale cultures described below, and the resulting EtOAc extracts tested in assays for cell proliferation/survival (MTT) and inhibition of metastatic cancer cell motility (WHA). *F. oxysporum* strain $EPH2R_{AA}$ was found to produce bioactive metabolites when cultured on PDA, whereas the strain CEC1S produced bioactive metabolites in PDB. Thus, for isolation of bioactive secondary metabolites, *F. oxysporum* $EPH2R_{AA}$ was cultured on PDA in 80 T-flasks (135 mL of PDA each) for 14 days at 28 °C, while the strain CEC1S was cultured in 12 L of PDB in six 4 L flasks (2 L of PDB each) on a shaker (150 rpm) for 14 days at 28 °C.

Extraction and Isolation of the Metabolites from *F. oxysporum* $EPH2R_{AA}$. After 14 days of cultivation, MeOH (200 mL/T-flask) was

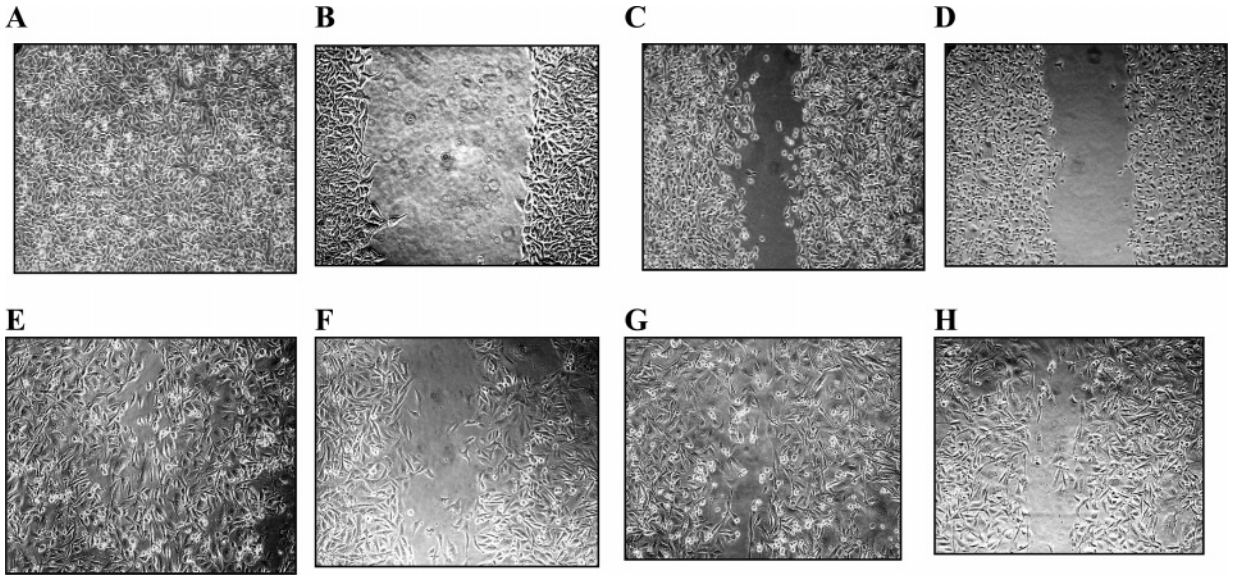

Figure 2. Wound-healing assay of beauvericin (**1**) with metastatic cancer cells PC-3M (A−D) and MDA-MB-231 (E−H). (A and E) DMSO control (negative). (B and F) LY294002 control (positive) at 7.5 μM. (C) Beauvericin at 2.0 μM. (D) Beauvericin at 2.5 μM. (G) Beauvericin at 3.0 μM. (H) Beauvericin at 4.0 μM.

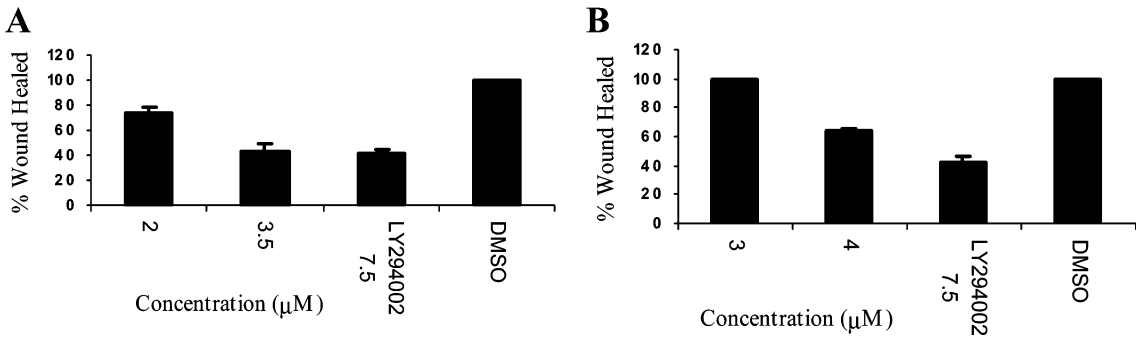

Figure 3. Quantitative wound-healing assay data for beauvericin (**1**). (A) In metastatic prostate cancer (PC-3M) cells. (B) In metastatic breast cancer (MDA-MB-231) cells.

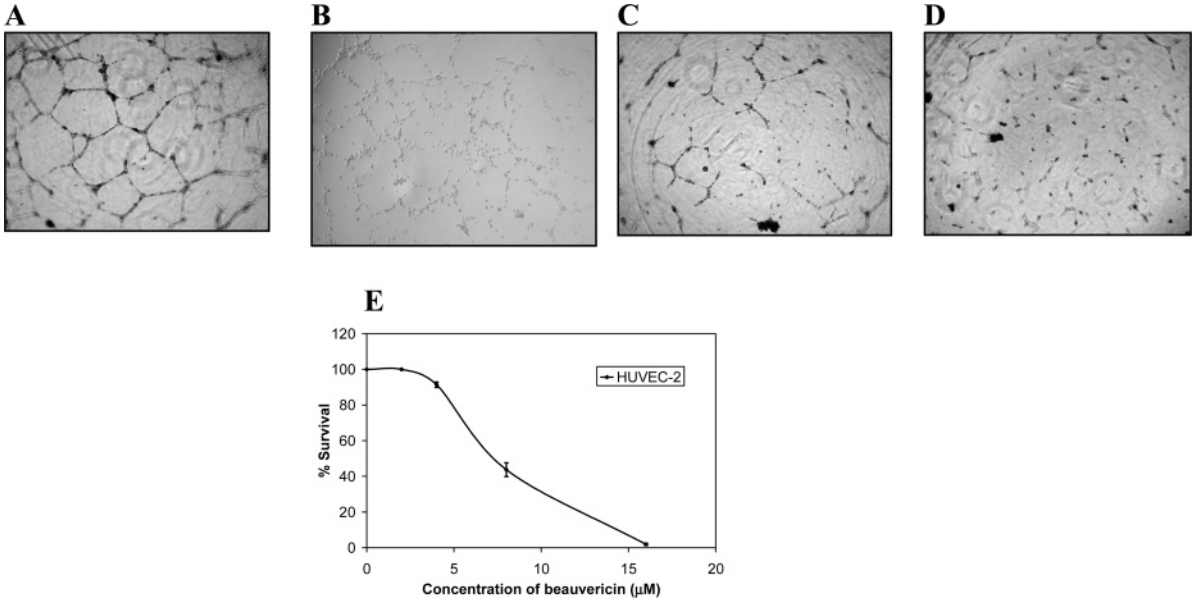

Figure 4. In vitro antiangiogenesis and cell survival assay of beauvericin (**1**) in HUVEC-2 cells exposed for 16 h. (A) Negative (DMSO) control. (B) Positive (withaferin A) control at 1.0 μM. (C) Beauvericin at 2.0 μM. (D) Beauvericin at 3.0 μM. (E) MTT cell survival assay ($n = 3$).

added to all 80 T-flasks and shaken in a rotary shaker for 8 h at 27 °C, and the resulting extract was filtered through Whatman No. 1 filter paper and a layer of Celite 545. The filtrate was concentrated to one-fourth of its original volume and extracted with EtOAc (3 × 1500 mL). Combined EtOAc extracts were evaporated under reduced pressure to afford a dark brown solid (696 mg), which showed activity in both

WHA and MTT assays. A portion of this extract (595 mg) was partitioned between hexane and 80% aqueous MeOH. The WHA-active aqueous MeOH fraction was diluted to 50% aqueous MeOH with water and extracted with $CHCl_3$. Of the resulting fractions, only the $CHCl_3$ fraction (322 mg) was found to be active, and this was subjected to size-exclusion chromatography on a column of Sephadex LH-20 (12 g) made up in hexane/CH_2Cl_2 (1:1) and eluted with hexane/CH_2Cl_2 (1:4) (100 mL), CH_2Cl_2/acetone (3:2) (100 mL), CH_2Cl_2/acetone (1:4) (100 mL), CH_2Cl_2/MeOH (1:1) (50 mL), and finally MeOH (50 mL). Twenty fractions were collected and combined into six fractions (F1−F6) on the basis of their TLC profiles, of which fractions F1 (110.9 mg) and F2 (71.2 mg) were found to be active. These two fractions were combined, and the combined fraction (F7) was fractionated further on a reversed-phase silica gel (RP-18; 6.0 g) column by elution with increasing amounts of MeOH (66%−100%) in H_2O, from which 11 fractions (F7A−F7K) were collected. Fractions F7E (23.4 mg), F7F (25.4 mg), and F7G (22.2 mg) were combined and further separated by reversed-phase preparative TLC (5% H_2O in MeOH), leading to the isolation of **1** (62.3 mg) and **4** (1.3 mg). Fraction F7D (35.2 mg) was separated by silica gel preparative TLC (hexane/acetone, 2:5) to yield **2** (10.5 mg) and **3** (6.6 mg).

Beauvericin (1): colorless needles (MeOH); mp 92−93 °C (lit.[15a] mp 93−94 °C); ^{1}H NMR (500 MHz, $CDCl_3$) δ 7.14−7.26 (5H, m), 5.45 (1H, dd, J = 11.1, 4.1 Hz), 4.91 (1H, d, J = 8.6 Hz), 3.34 (1H, dd, J = 14.6, 5.0 Hz), 2.98 (3H, s), 2.97 (1H, dd, J = 14.6, 11.8 Hz), 2.00 (1H, m), 0.79 (3H, d, J = 6.7 Hz), 0.42 (3H, d, J = 6.8 Hz); APCIMS (+) mode m/z 784 $[M + 1]^+$.

(−)-Oxysporidinone (2): colorless, amorphous solid; $[\alpha]_D^{25}$ −101.1 (c 0.20, MeOH); ^{1}H and ^{13}C NMR data, see Tables 1 and 2; APCIMS (+) mode m/z 490 $[M + 1]^+$; APCIMS (−) mode m/z 488 $[M - 1]^+$.

(−)-4,6′-Anhydrooxysporidinone (3): colorless crystalline solid (MeOH); mp 160−161 °C; $[\alpha]_D^{25}$ −78.6 (c 0.30, MeOH); UV (MeOH) λ_{max} (log ϵ) 290.2 (3.70) nm; IR (KBr) ν_{max} 3406, 3215, 2958, 2924, 2872, 1724, 1703, 1668, 1593, 1564, 1456, 1136, 1065, 1013 cm^{-1}; ^{1}H and ^{13}C NMR data, see Tables 1 and 2; APCIMS (+) mode m/z 472 $[M + 1]^+$; APCIMS (−) mode m/z 470 $[M - 1]^+$; HRFABMS m/z 472.3062 $[M + 1]^+$ (calcd for $C_{28}H_{42}NO_5$, 472.3063).

(−)-6-Deoxyoxysporidinone (4): colorless, crystalline solid; mp 130−131 °C; $[\alpha]_D^{25}$ −72.0 (c 0.15, MeOH); UV (MeOH) λ_{max} (log ϵ) 219.8 (4.46), 296.0 (3.66) nm; IR (KBr) ν_{max} 3418, 3234, 2959, 2924, 2872, 1705, 1651, 1564, 1445, 1383, 1065, 1013 cm^{-1}; ^{1}H and ^{13}C NMR data, see Tables 1 and 2; APCIMS (+) mode m/z 474 $[M + 1]^+$; APCIMS (−) mode m/z 472 $[M - 1]^+$; HRFABMS m/z 474.3242 $[M + 1]^+$ (calcd for $C_{28}H_{44}NO_5$, 474.3219).

Extraction and Isolation of the Metabolites from *F. oxysporum* CEC1S. After 14 days of fermentation, the PDB culture was filtered through Whatman No. 1 filter paper, and the filtrate (12 L; pH = 4.4) neutralized with 1 N NaOH and extracted (× 3) with EtOAc (10 L). The EtOAc extract thus obtained was evaporated under reduced pressure to obtain a dark red solid (603 mg), which was found to be active in the MTT assay. Solvent−solvent partitioning of a portion (552 mg) of this EtOAc extract as for *F. oxysporum* EPH2R$_{AA}$ above afforded hexane (20.1 mg), $CHCl_3$ (276 mg), and 50% aqueous MeOH (245 mg) fractions, of which the latter two fractions were found to be active in the MTT assay. A portion (261 mg) of the $CHCl_3$ fraction was subjected to size-exclusion chromatography on Sephadex LH-20 and eluted with hexane/CH_2Cl_2 (1:4) (100 mL), CH_2Cl_2/acetone (2:3) (100 mL), CH_2Cl_2/acetone (1:4) (100 mL), CH_2Cl_2/MeOH (1:1) (100 mL), and finally MeOH (100 mL), yielding five fractions, F1′ (129.5 mg), F2′ (71.9 mg), F3′ (25.1 mg), F4′ (16.4 mg), and F5′ (14.7 mg). All five fractions were active in the MTT assay and were found to have common TLC spots, including those due to a major red compound and a minor yellow compound. These fractions and the 50% aqueous MeOH fraction active in the MTT assay were separately subjected to silica gel preparative TLC (CH_2Cl_2/MeOH, 92:8), and the resulting fractions with the same R_f were combined, affording **6** (58.1 mg; R_f = 0.6) and **7** (1.5 mg; R_f = 0.8). Similar fractionation of F3′ provided **5** (2.9 mg; R_f = 0.2) together with small quantities of **6** and **7**.

Rhodolamprometrin (5): orange powder; ^{1}H NMR (500 MHz, DMSO-d_6) δ 12.4 (1H, s, 1-OH), 12.1 (1H, s, 8-OH), 7.04 (1H, d, J = 1.7 Hz, H-5), 6.59 (1H, d, J = 1.7 Hz, H-7), 6.63 (1H, s, H-2), 2.37 (3H, s, 4-COCH$_3$); APCIMS (−) mode m/z 314 $[M]^+$. Its NMR and MS data were consistent with those reported for rhodolamprometrin.[21]

Bikaverin (6): red powder; ^{1}H NMR (500 MHz, $CDCl_3$) δ 6.90 (1H, d, J = 2.5 Hz, H-4), 6.78 (1H, d, J = 2.5 Hz, H-2), 6.33 (1H, s, H-9), 3.94 (3H, s, 8-OCH$_3$), 3.91 (3H, s, 3-OCH$_3$), 2.84 (3H, s, 1-CH$_3$); APCIMS (+) mode m/z 383 $[M + 1]^+$. These NMR and MS data compared well with those reported for bikaverin.[22]

6-Deoxybikaverin (7): yellow powder; ^{1}H NMR (500 MHz, $CDCl_3$) δ 7.61 (1H, s, H-6), 6.75 (2H, d, J = 2.5 Hz, H-2 and H-4), 6.16 (1H, s, H-9), 3.92 (3H, s, 8-OCH$_3$), 3.88 (3H, s, 3-OCH$_3$), 2.85 (3H, s, 1-CH$_3$); APCIMS (+) mode m/z 367 $[M + 1]^+$. These NMR and MS data were consistent with those reported in the literature.[23]

Cytotoxicity Assay. The tetrazolium-based colorometric assay (MTT assay)[13] was used for the in vitro assay of cytotoxicity to NCI-H460 (non-small-cell lung cancer), MIA Pa Ca-2 (pancreatic carcinoma), MCF-7 (breast cancer), and SF-268 (CNS glioma). Doxorubicin and DMSO were used as positive and negative controls.

Wound-Healing Assay (WHA). For WHA the metastatic prostate cancer (PC-3M) cells were cultured in RPMI 1640 medium containing 10% fetal bovine serum, penicillin (100 IU/mL), and streptomycin (50 μg/mL), and the metastatic breast cancer (MDA-MB-231) cells were cultured in DMEM/Ham's F-12 medium containing 10% fetal bovine serum and gentamycin (50 μg/mL). Both types of cells were grown in a 5% CO_2 atmosphere at 37 °C, and the cells were harvested at or above 80% confluence. The cells were plated onto sterile 24-well plates at a density of 70 000 cells per well for PC-3M and 150 000 cells per well for MDA-MB-231 and were allowed to recover for 48 and 24 h, respectively, until a confluent cell monolayer had formed in each well (>90% confluence). Wounds were then inflicted to each cell monolayer using a sterile toothpick, media were removed, the cell monolayers were washed once with PBS, and fresh media were added to each well. Test samples (extracts, fractions, or beauvericin) were prepared in DMSO at different concentrations and added to the plates, each in duplicate along with the two controls, phosphotidylinositol (PtdIns) 3-kinase inhibitor LY294002[29] at 7.5 μM (positive control) and DMSO (negative control). The plates were incubated for 40 h (PC-3M) or 20 h (MDA-MB-231), during which the wells treated with DMSO had healed entirely and the wells treated with LY294002 and samples containing cell motility inhibitors had wounds present. All treatments, including the controls, were documented photographically. A treatment was considered active if there was a wound present in duplicate wells at the completion of the assay.

Quantification of Wound-Healing Inhibition. ImageJ software, available from the NIH website (http://rsb.info.nih.gov/rj/), was used to quantify WHA data.[27] Three random pictures were taken for each wound using an inverted microscope at 20× magnification; photos were taken immediately after a wound was inflicted to the cell monolayer and uploaded into the ImageJ software, the area of the wound was measured by using the rectangle area selection tool, and the three areas per well were averaged. After the DMSO wells had healed (usually 40 h after infliction of the wound for PC-3M and 20 h for MDA-MD-231), three random pictures were taken for each treated well and the areas of the wounds measured as above. The % of wound healed was then calculated using the formula 100 − (final area/initial area × 100%).[27]

In Vitro Angiogenesis Assay. Matrigel (BD Biosciences) was placed in sterile round-bottomed 96-well plates (45 μL of Matrigel per well). Once the Matrigel had formed into a gel, HUVEC-2 cells cultured in EBM Basal Medium supplemented with EGM-MV SingleQuot kit (Cambrex Bio Science Walkersville, Inc) were plated onto the Matrigel at a density of 10 000 cells per well and were allowed to adhere to the gel (adherence occurs in ca. 1 h). After the cells had adhered to the Matrigel, DMSO (negative control), 1.0 μM withaferin A (positive control),[7] and various concentrations of beauvericin (**1**) in the above media were added to separate wells (in triplicate). The plates were incubated overnight (ca. 16 h), and the results were documented photographically using an inverted microscope at 4× magnification and were edited in Microsoft Office Picture Manager.

Acknowledgment. Financial support for this work was provided by Grant R01 CA 90265 funded by the National Cancer Institute, and Contract 0013 awarded by Arizona Biomedical Research Commission. We thank S. Wittlinger, C. Hamilton, L. Morse, C. Hayes, and A. Das (Arizona State University) for their assistance in the collection, isolation, and identification of the fungal strains used in this work, C. J. Seliga and L. A. Luevano (University of Arizona), respectively, for their

assistance in large-scale culturing of the fungus and preliminary wound-healing assays, and Drs. N. Jacobsen and K. Wijeratne (University of Arizona) for the HMBC spectrum of **3** on the Varian Inova-600. Dr. D. Nanayakkara (University of Mississippi) is thanked for providing copies of spectroscopic data for (−)-oxysporidinone.

References and Notes

(1) Studies on Arid Lands Plants and Microorganisms, Part 13. For Part 12, see: Bashyal, B. P.; McLaughlin, S. P.; Gunatilaka, A. A. L. *J. Nat. Prod.* **2006**, *69*, 1820−1822.
(2) Fenteany, G.; Zhu, S. *Curr. Top. Med. Chem.* **2003**, *3*, 593−616.
(3) Sporn, M. B. *Lancet* **1996**, *347*, 1377−1381.
(4) Carmeliet, P. *Nat. Med.* **2003**, *9*, 653−660.
(5) Gaul, C.; Njardarson, J. T.; Shan, D.; Dorn, D. C.; Wu, K. D.; Tong, W. P.; Huang, X. Y.; Moore, M. A. S.; Danishefsky, S. J. *J. Am. Chem. Soc.* **2004**, *126*, 11326−11337.
(6) Kielbassa, K.; Schmitz, C.; Gerke, V. *Exp. Cell Res.* **1998**, *243*, 129−141.
(7) Falsey, R. R.; Marron, M. T.; Gunaherath, G. M. K. B.; Shirahatti, N.; Mahadevan, D.; Gunatilaka, A. A. L.; Whitesell, L. *Nat. Chem. Biol.* **2006**, *2*, 33−38.
(8) (a) Han, S. B.; Kim, H. M.; Kim, Y. H.; Lee, C. W.; Jang, E. S.; Son, K. H.; Kim, S. U.; Kim, Y. K. *Int. J. Immunopharmacol.* **1998**, *20*, 1−13. (b) Zhang, J.; Shen, Y.; Liu, J.; Wei, D. *Biochem. Pharmacol.* **2005**, *69*, 407−414.
(9) Nakae, K.; Yoshimoto, Y.; Sawa, T.; Homma, Y.; Hamada, M.; Takeuchi, T.; Imoto, M. *J. Antibiot.* **2000**, *53*, 1130−1136.
(10) Roskelley, C. D.; Williams, D. E.; McHardy, L. M.; Leong, K. G.; Troussard, A.; Karsan, A.; Anderson, R. J.; Dedhar, S.; Roberge, M. *Cancer Res.* **2001**, *61*, 6788−6794.
(11) Yarrow, J. C.; Totsukawa, G.; Charras, G. T.; Mitchison, T. J. *Chem. Biol.* **2005**, *12*, 385−395.
(12) (a) Gusman, J.; Vanhaelen, M. *Recent Res. Dev. Phytochem.* **2000**, *4*, 187−206. (b) Tan, R. X.; Zou, W. X. *Nat. Prod. Rep.* **2001**, *18*, 448−459. (c) Schulz, B.; Boyle, C.; Draeger, S.; Rommert, A.-K.; Krohn, K. *Mycol. Res.* **2002**, *106*, 996−1004. (d) Strobel, G. A. *Crit. Rev. Biotech.* **2002**, *22*, 315−333. (e) Strobel, G. A. *Microbes Infect.* **2003**, *5*, 535−544. (f) Strobel, G.; Daisy, B. *Microbiol. Mol. Biol. Rev.* **2003**, *67*, 491−502. (h) Strobel, G.; Daisy, B.; Castillo, U.; Harper, J. *J. Nat. Prod.* **2004**, *67*, 257−268. (i) Gunatilaka, A. A. L. *J. Nat. Prod.* **2006**, *69*, 509−526.
(13) Rubinstein, L. V.; Shoemaker, R. H.; Paul, K. D.; Simon, R. M.; Tosini, S.; Skehan, P.; Sudiero, D. A.; Monks, A.; Boyd, M. R. *J. Nat. Cancer Inst.* **1990**, *82*, 1113−1118.
(14) (a) Seo, J. A.; Kim, J. C.; Lee, Y. W. *J. Nat. Prod.* **1999**, *62*, 355−357. (b) Seo, J. A.; Kim, J. C.; Lee, Y. W. *J. Nat. Prod.* **1996**, *59*, 1003−1005. (c) Kim, J. C.; Lee, Y. W. *Appl. Environ. Microbiol.* **1994**, *60*, 4380−4386. (d) Breinholt, J.; Ludvigsen, S.; Rassing, B. R.; Rosendahl, C. N.; Nielsen, S. E.; Olsen, C. E. *J. Nat. Prod.* **1997**, *60*, 33−35. (e) Rodriguez, M. A.; Cabrera, G.; Godeas, A. *J. Appl. Microbiol.* **2006**, *100*, 575−586. (f) Jayasinghe, L.; Abbas, H. K.; Jacob, M. R.; Herath, W. H. M. W.; Nanayakkara, N. P. D. *J. Nat. Prod.* **2006**, *69*, 439−442.
(15) (a) Hamill, R. L.; Higgens, C. E.; Boaz, H. E.; Gorman, M. *Tetrahedron Lett.* **1969**, *49*, 4255−4258. (b) Bernardini, M.; Carilli, A.; Pacioni, G.; Santurbano, B. *Phytochemistry* **1975**, *14*, 1865. (c) Deol, B. S.; Ridley, D. D.; Singh, P. *Aust. J. Chem.* **1978**, *31*, 1397−1399.
(16) (a) Gupta, S.; Krasnoff, S. B.; Underwood, N. L.; Renwick, J. A. A.; Roberts, D. W. *Mycopathologia* **1991**, *115*, 185−189. (b) Moretti, A.; Belisario, A.; Tafuri, A.; Ritieni, A.; Corazza, L.; Logrieco, A. *Eur. J. Plant Pathol.* **2002**, *108*, 661−666.
(17) Ivanova, L.; Skjerve, E.; Eriksen, G. S.; Uhlig, S. *Toxicon* **2006**, *47*, 868−876.
(18) Tomoda, H.; Huang, X. H.; Cao, J.; Nishida, H.; Nagao, R.; Okuda, S.; Tanaka, H.; Omura, S.; Arai, H.; Inoue, K. *J. Antibiot.* **1992**, *45*, 1626−1632.
(19) Jow, G.-M.; Chou, C.-J.; Chen, B.-F.; Tsai, J.-H. *Cancer Lett.* **2004**, *216*, 165−173.
(20) Fuska, J.; Proska, B.; Fuskova, A. *Neoplasma* **1975**, *22*, 335−338.
(21) Betina, V.; Sedmera, P.; Vokoun, J.; Podojil, M. *Experientia* **1986**, *42*, 196−197.
(22) Kjær, D.; Kjær, A.; Pedersen, C.; Bu'Lock, J. D.; Smith J. R. *J. Chem. Soc.* **1971**, 2792−2797.
(23) Kjær, D.; Kjær, A.; Risbjerg, E. *J. Chem. Soc., Perkin Trans. 1* **1983**, 2815−2820.
(24) Erdman, T. R.; Thomson, R. H. *J. Chem. Soc.* **1972**, 1291−1292.
(25) (a) Chelkowski, J.; Zajkowski, P.; Visconti, A. *Mycotoxin Res.* **1992**, *8*, 73−76. (b) Jones, A.; Pharis, R. P. *J. Ferment. Technol.* **1987**, *65*, 717−722. (c) Brewer, D.; Arsenault, G. P.; Wright, J. L. C.; Vining, L. C. *J. Antibiot.* **1973**, *26*, 778−781. (d) Cornforth, J. W.; Ryback, G.; Robinson, P. M.; Park, D. *J. Chem. Soc.* **1971**, 2786−2788. (e) Balan, J.; Fuska, J.; Kuhr, I.; Kuhrova, V. *Folia Microbiol.* **1970**, *15*, 479−484.
(26) Terashima, N.; Ishida, M.; Hamasaki, T.; Hatsuda, Y. *Phytochemistry* **1972**, *11*, 2880.
(27) Ehlers, J. P.; Worley, L.; Onken, M. D.; Harbour, J. W. *Clin. Cancer Res.* **2005**, *11*, 3609−3613.
(28) (a) Zhang, H.-T.; Bicknell, R. In *Angiogenesis Protocols*; Murray, J. C., Ed.; Humana Press: Totowa, NJ, 2001; Chapter 1, pp 3−26. (b) Meade-Tollin, L. C.; Wijeratne, E. M. K.; Cooper, D.; Guild, M.; Jon, E.; Fritz, A.; Zhou, G.-X.; Whitesell, L.; Liang, J.-Y.; Gunatilaka, A. A. L. *J. Nat. Prod.* **2004**, *67*, 2−4.
(29) Vlahos, C. J.; Matter, W. F.; Hui, K. Y.; Brown, R. F. *J. Biol. Chem.* **1994**, *269*, 5241−5248.

NP060394T